

PREPARED FOR THE U.S. DEPARTMENT OF ENERGY,
UNDER CONTRACT DE-AC02-76CH03073

PPPL-3554
UC-70

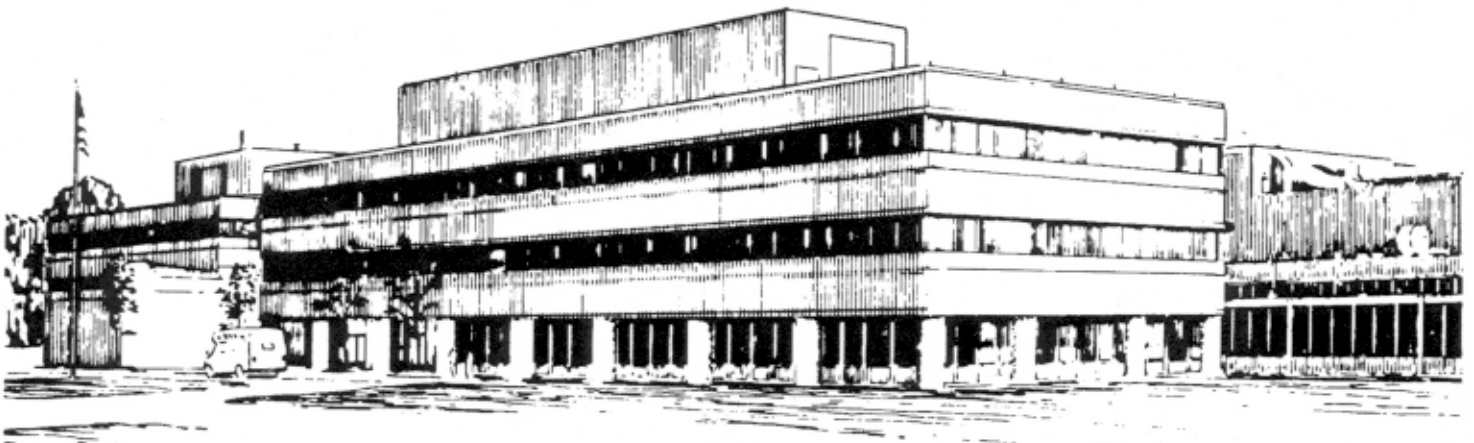
PPPL-3554

**Electron Acceleration in the Field-reversed Configuration (FRC)
by Slowly Rotating Odd-parity Magnetic Fields (RMF)**

by

Alan H. Glasser and Samuel A. Cohen

April 2001



**PRINCETON PLASMA PHYSICS LABORATORY
PRINCETON UNIVERSITY, PRINCETON, NEW JERSEY**

PPPL Reports Disclaimer

This report was prepared as an account of work sponsored by an agency of the United States Government. Neither the United States Government nor any agency thereof, nor any of their employees, makes any warranty, express or implied, or assumes any legal liability or responsibility for the accuracy, completeness, or usefulness of any information, apparatus, product, or process disclosed, or represents that its use would not infringe privately owned rights. Reference herein to any specific commercial product, process, or service by trade name, trademark, manufacturer, or otherwise, does not necessarily constitute or imply its endorsement, recommendation, or favoring by the United States Government or any agency thereof. The views and opinions of authors expressed herein do not necessarily state or reflect those of the United States Government or any agency thereof.

Availability

This report is posted on the U.S. Department of Energy's Princeton Plasma Physics Laboratory Publications and Reports web site in Calendar Year 2001. The home page for PPPL Reports and Publications is: http://www.pppl.gov/pub_report/

DOE and DOE Contractors can obtain copies of this report from:

U.S. Department of Energy
Office of Scientific and Technical Information
DOE Technical Information Services (DTIS)
P.O. Box 62
Oak Ridge, TN 37831

Telephone: (865) 576-8401

Fax: (865) 576-5728

Email: reports@adonis.osti.gov

This report is available to the general public from:

National Technical Information Service
U.S. Department of Commerce
5285 Port Royal Road
Springfield, VA 22161

Telephone: 1-800-553-6847 or
(703) 605-6000

Fax: (703) 321-8547

Internet: <http://www.ntis.gov/ordering.htm>

Electron acceleration in the field-reversed configuration (FRC) by slowly rotating odd-parity magnetic fields (RMF_o)

Alan H. Glasser, Los Alamos National Laboratory, Los Alamos, NM 87545
Samuel A. Cohen, Princeton Plasma Physics Laboratory, Princeton, NJ 08543

Abstract

The trajectories of individual electrons are studied numerically in a 3D, prolate, FRC equilibrium magnetic geometry with added small-amplitude, slowly rotating, odd-parity magnetic fields (RMF_os). RMF_os cause electron heating by toroidal acceleration near the O-point line and by field-parallel acceleration away from it, both followed by scattering from magnetic-field inhomogeneities. Electrons accelerated along the O-point line move antiparallel to the FRC's current and attain average toroidal angular speeds near that of the RMF_o, independent of the sense of RMF_o rotation. A conserved transformed Hamiltonian, dependent on electron energy and RMF_o sense, controls electron flux-surface coordinate.

A recent publication¹ considered the orbits of individual ions in an FRC with small-amplitude odd-parity² rotating magnetic fields (RMF_os) in the Ion Cyclotron Range of Frequencies (ICRF). That paper showed that ions can be accelerated to thermonuclear energies in a modest-size device without loss of confinement. In this paper we study the motion of electrons in the same system, with the RMF_o still in the ICRF, far below the electron cyclotron frequency range. Because of the mass difference, the physical mechanisms responsible for electron heating are far different from those described for the ions whose heating can be viewed as a hybrid of cyclotron resonance and Fermi acceleration. In contrast, the physical picture of electron heating combines acceleration by slowly-varying electric fields with scattering from field inhomogeneities. We show that this essential difference results in novel phenomena. All other conditions noted in Ref.1 also apply here.

These results are important for fusion reactor design. The FRC, recognized to have many attractive technical and scientific features as a power plant,³ lacks proven methods to heat electrons and drive sustained currents, particularly on the magnetic axis.⁴⁻⁷ This paper shows the physics by which RMF_os in the ICRF can heat electrons and drive an on-axis electron current.

A central feature of the electron-heating mechanism is collisionless scattering from the non-uniform magnetic field structure, first described by Speiser in 2-D.⁸ In an FRC with elongation $\kappa \equiv z_s/r_s$, (r_s = separatrix radius and $\pm z_s$ = axial positions of the X points), the magnetic field strength $|B|$ drops by a factor $\geq 2\kappa$ in going from the mid-plane to the extrema of a flux surface. As the electron approaches the sharp curve at an extremum, its gyro-radius, ρ_L , increases and the radius of field curvature, r_c decreases. If $\rho_L/r_c > 0.01$, the adiabatic invariance of magnetic moment is violated where the field reverses direction; the energy is equipartitioned between parallel and perpendicular motions. In this scattering, no shift in the electron's flux-surface coordinate occurs. Our simulations, performed in 3-D, show new phenomena.

In the computer code, RMF_{1.13}, we use an adaptive integrator⁹ to integrate the six coupled nonlinear ordinary differential equations comprising Hamilton's equations,¹⁰

$$\dot{q}_i = \partial H / \partial p_i, \quad \dot{p}_i = -\partial H / \partial q_i, \quad i = r, z, \phi \quad (1)$$

with H the Hamiltonian and q_i and p_i the canonical coordinates and momenta. Vector potentials for the Solov'ev FRC¹¹ and the RMF_os¹ are respectively given by

$$rA_{\phi, \text{FRC}} \equiv \Psi_{\text{FRC}} = \Psi_0(r^2/r_s^2)(1 - r^2/r_s^2 - z^2/z_s^2), \quad (2)$$

$$\{A_r, A_z, A_\phi\}_{\text{odd}} = (2B_R/k) \{I_0(\xi) \cos kz \sin \psi, -I_1(\xi) \sin kz \sin \psi, I_0(\xi) \cos kz \cos \psi\}, \quad (3)$$

with $\Psi_0 = B_a r_s^2 / 2$, B_a the FRC field at $z = r = 0$, B_R the RMF_o field amplitude, $k = l\pi/\kappa r_s$ the RMF_o wave number, l the RMF_o axial mode number, $\xi \equiv kr$, m_e the electron mass, $q_e = -e$ the electron charge, $\psi \equiv \phi - \omega_R t$, $\omega_{ce} \equiv q_e B_a / m_e c$ the electron cyclotron frequency, ω_R the RMF_o frequency, and I_m modified Bessel functions. An electrostatic potential $\varphi(\Psi_{\text{FRC}})$ may be included in H , as suggested by fluid models.¹² We have studied φ values up to 10 keV and seen that the primary results are unaltered. For simplicity, all results reported here had $\varphi = 0$.

Because H depends on ϕ and t only through ψ , it follows that the transformed Hamiltonian

$$K \equiv H - \omega_R p_\phi \quad (4)$$

is conserved.¹⁰ K is used to monitor the accuracy of numerical integration and, more importantly, is shown below to control electron motion across flux surfaces.

In a typical RMF_{1.13} run, a 100-eV electron is initialized at a position inside the FRC's separatrix. Other initial parameters are the angles of the electron's velocity, and the mode structure, phase, frequency, and amplitude of the RMF_o. Electrons with 100 eV perform cyclotron orbits, unless they are very close to the O-point null line, in which case they may perform null-line-crossing betatron orbits.^{13,14} In an FRC, electron cyclotron orbits drift in one toroidal direction, parallel to the FRC's current, thus reducing it, while betatron orbits move in the opposite direction, adding to the current. The sign of ω_R is positive when the RMF_o rotates in the direction of the electron betatron motion.

For the reference FRC (RFRC) of Ref. 1, with $B_a = 2 \times 10^4$ G, $r_s = 10$ cm, and $\kappa = 5$, Fig. 1 shows results of an RMF_{1.13} simulation for an electron initiated on a flux surface near the O-point line. The RMF_o parameters were $\omega_R/\omega_{ce} = 2 \times 10^{-4}$ and $B_R = 20$ G. This sense of RMF_o rotation, positive ω_R/ω_{ce} , is the same as known to drive current for even-parity RMF (RMF_e). The electron energy is shown as a function of $\tau = t/\tau_{ce}$, time measured in units of the electron cyclotron period $\tau_{ce} = 2\pi/\omega_{ce}$ at B_a . The energy periodically spikes to above 4 keV and then nearly returns to its pre-spike baseline value. A slow, secular increase in the baseline energy also occurs, reaching a maximum of about 2 keV at $\tau \approx 4 \times 10^4$. As the baseline energy rises, the heights of the spikes above the baseline decrease; the maximum energy attained (spikes *plus* baseline) also decreases. Extending the simulation to $\tau = 10^7$ resulted in less than a 3% further increase in maximum energy attained. In this extended time period, the secular behavior of the baseline energy is not

monotonic; its value varies between zero and about 3 keV. Numerical integration of the energy gain $\Delta\mathcal{E} \equiv \int_0^t q_e \mathbf{E} \cdot \mathbf{v}_e dt$ shows that both the energy spikes and the secular energy gain come predominantly from the azimuthal (toroidal) component E_ϕ .

Figure 2 shows, with finer time resolution, the same electron's energy, axial position z , radial position r , and azimuthal position, ϕ . The spikes occur during betatron-type orbits, when the electron is near the O-point position, $r = 7.07$ cm, $z = 0$ cm. The results of Speiser collisions can be seen, Fig. 2b, in the erratic motion near the z *extrema* of the original flux surface, $\sim \pm 4$ cm. For example, numerous Speiser collisions occur during the interval $3700 < \tau < 5500$, causing the electron to linger near the positive z *extremum*. The ϕ position, Fig. 2d, becomes increasingly more negative with τ , dominated by steps due to the energetic betatron orbits. The time-averaged angular velocity $\langle \dot{\phi} \rangle$ has the same rotation sense as the RMF_o and nearly (0.98) the same magnitude. This time-averaged synchronous motion continues for very long times, beyond $\tau = 10^7$. Electrons accelerated with a positive ω_R/ω_{ce} RMF_o are well confined; they move towards the O point with increasing energy. Electrons initiated away from the O point are accelerated to high energy by the E_z field; Speiser collisions cause isotropization of the energy. These electrons move towards the O point where the E_ϕ field can cause toroidal acceleration. As we show later, electrons initiated further from the O point eventually attain higher energy than those initiated nearer the O point.

Figure 3 shows $\text{RMF}_{1.13}$ results for reversed rotation, $\omega_R/\omega_{ce} = -2 \times 10^{-4}$. Energy spikes of \sim half the amplitude as for positive ω_R/ω_{ce} occur during the early phase, $\tau < 3 \times 10^4$. Surprisingly, for this reversed RMF_o rotation direction, the electron initially moves with nearly the same average toroidal angular speed (Fig. 3b) as the RMF_o , but with the opposite rotational sense, contrary to the commonly invoked physical picture of electrons frozen to the rotating magnetic field.^{14–16} At times when the energy is above ~ 5 keV, the spikes are absent.

For negative ω_R/ω_{ce} , electrons accelerated to higher energies move further away from the O point. The further an electron moves from the O point, the larger the fraction of its total kinetic energy, \mathcal{E}_t , comes from E_z . At larger energies and smaller values of Ψ_{FRC} , the average toroidal angular speed of an electron is a very small fraction of ω_R , Fig. 3b. Because of this outward motion with increasing energy, the energy of those electrons initiated near the O point eventually increases to much above that obtained for the same initial position with $\omega_R/\omega_{ce} = +2 \times 10^{-4}$, to about 10 keV at $\tau = 10^5$ and 40 keV at $\tau = 10^6$.

That electrons heated at negative ω_R/ω_{ce} move away from the O point while those heated at positive ω_R/ω_{ce} move towards the O point can be understood from the constancy of K , Eq. (4). The dominant part of $p_\phi = mr^2\dot{\phi} + q_e r A_\phi/c$ is $q_e \Psi_{\text{FRC}}/c$. A change of the sign of ω_R/ω_{ce} requires a corresponding change of sign of the time derivative of Ψ_{FRC} to conserve K with changing H .

The energy spikes can be understood in terms of the combined effects of the FRC's static magnetic field and the time-dependent RMF_o -generated electric field. Because the FRC has a minimum-B geometry with $B = 0$ at the O point, $r = r_o$ and $z = 0$, an electron there is guided toroidally around the FRC in a near-circular orbit of radius $r = r_o$,

with small axial and radial betatron modulations.^{13,14} The RMF_o produces an azimuthal electric field *via* the time derivative $-(\partial A_{\phi,odd}/\partial t)/c$ of Eqn. (3), causing the electron to accelerate azimuthally. The $\cos\psi$ term in $A_{\phi,odd}$, Eq. (3), causes the electric field to reverse sign twice as ϕ increases by 2π . A sufficiently fast electron will proceed in this field to where the E_ϕ field reverses direction, i.e., about half way around the FRC. At that point, deceleration will begin and proceed until nearly all the energy gained is lost. If a non-adiabatic scattering event occurs before all the energy is lost, heating occurs. Energy spikes occur for both directions of RMF_o rotation because both produce an E_ϕ with the same toroidal behavior. Energy spikes are larger for positive ω_R/ω_{ce} because the RMF_o rotates in the direction of the betatron orbits so electrons stay longer in phase with the E_ϕ than for negative ω_R/ω_{ce} .

From a series of over 2000 RMF_{1.13} runs, we determine how the maximum energy \mathcal{E}_{\max} attained by an electron depends on its initial position r_{init} , the strength and frequency of the RMF_o, the rotation sense of the RMF_o, and the duration of the RMF_{1.13} run. For $\omega_R/\omega_{ce} = 2 \times 10^{-4}$, Fig. 4a shows, for four strengths of RMF_o, the maximum energy attained in time $\tau = 5 \times 10^4$ as a function of r_{init} , normalized to the O-point radius, $\rho_{\text{init}} \equiv r_{\text{init}}/r_o$. At $B_R = 1$ G, a peak in \mathcal{E}_{\max} appears at $\rho_{\text{init}} = 1$, exceeding the off-O-point heating by about a factor of 5. The height of \mathcal{E}_{\max} increases and the radial width, δ_p , of the near-O-point heating broadens with increasing B_R , ω_R , and τ , ($\delta_p \propto \tau^{0.2}$), but the central peak collapses. The smooth sunken peak that develops is a robust feature of RMF_{1.13} simulations for positive ω_R/ω_{ce} . It can be understood from Eq. 2 and 4. When ω_R/ω_{ce} is negative, a sunken peak in \mathcal{E}_{\max} does not occur because electrons initiated near the O point move to lower Ψ_{FRC} and are not restricted in energy by Eq. 4.; \mathcal{E}_{\max} is then roughly independent of ρ_{init} and equal to the value obtained with positive ω_R/ω_{ce} for electrons initiated at the separatrix radius.

The ratio $\alpha^* \equiv \langle \dot{\phi} \rangle / \omega_R$ is shown in Fig. 4b for positive ω_R/ω_{ce} as functions of B_R and ρ_{init} . (Positive α^* means electron azimuthal angular velocity in the same direction as the RMF_o rotation.) Synchronous rotation occurs in the same regions as the sunken peaks in Fig. 4a. The plateaus in α^* mark the initial positions of the electrons' trajectories, which is not the same as the regions where motion synchronous with the RMF_o occurs. Electrons move synchronously with the RMF_o only close to the O point, typically within $\pm 5\% r_o$ and $\pm 10\% z_s$.

Speiser scattering might be invoked to estimate a non-Ohmic resistivity, for example, by assuming that Speiser collisions occur each time an electron moves a distance $\sim \kappa r_s$ along the magnetic field. This simple model predicts that the ratio of Speiser collision frequency, ν_s , to the Spitzer collision frequency, ν_z , is $\nu_s/\nu_z \sim 10^{12} \mathcal{E}_e^2 / n_e r_s \kappa$. This could provide an explanation for the enhanced resistivity seen in both FRC⁴ and spheromak¹⁷ experiments. However, the results shown in Fig. 2 indicate that this model oversimplifies the resistivity, most clearly for RMF-heated FRCs, because the energy gain saturates for positive ω_R/ω_{ce} . For negative ω_R/ω_{ce} , \mathcal{E}_t grows slowly, $\propto \tau^{0.5}$.

In summary, we have shown with a full 3-D model that, if RMF_o penetration is full, small-amplitude odd-parity rotating magnetic fields can be used in modest-sized FRC devices to heat electrons to fusion-relevant energies. For the standard RMF_o rotation

sense, electrons initiated away from the O point are accelerated by the E_z field and their energy is redistributed amongst the degrees-of-freedom by Speiser collisions. The orbits of these electrons move towards the O point as their energy increases. Near the O point they are accelerated predominantly by the E_ϕ field, to synchronous motion with the RMF_o. For the opposite sense of RMF_o rotation, electrons near the magnetic axis are also accelerated to angular speeds equal to that of the RMF_o, but their sense of rotation is opposite. As these electrons heat, they move away from the O point and their toroidal drift speed decreases. The role of the conserved transformed Hamiltonian, K , in determining electron flux-surface coordinate is shown. These results are relevant to a compact magnetic-fusion-reactor design.

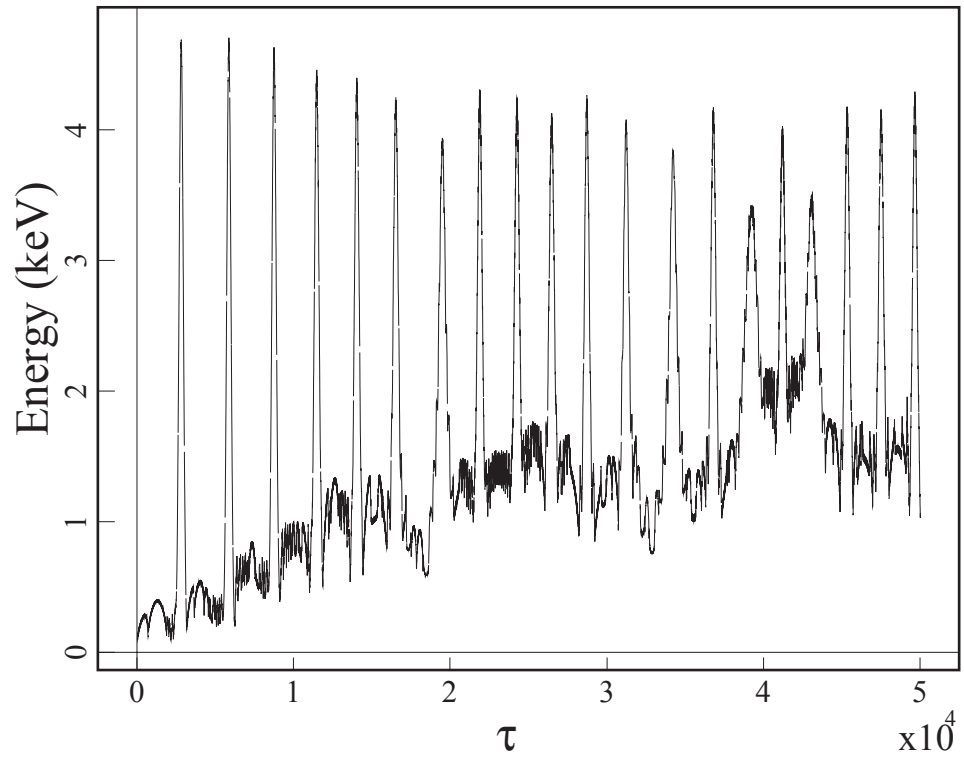
We thank T. Carter, T.K. Chu, J. Finn, J. Foley, T. Kornack and T. Munsat for useful discussions. This work was supported in part by U.S. Department of Energy Contract No. DE-AC02-76-CHO-3073.

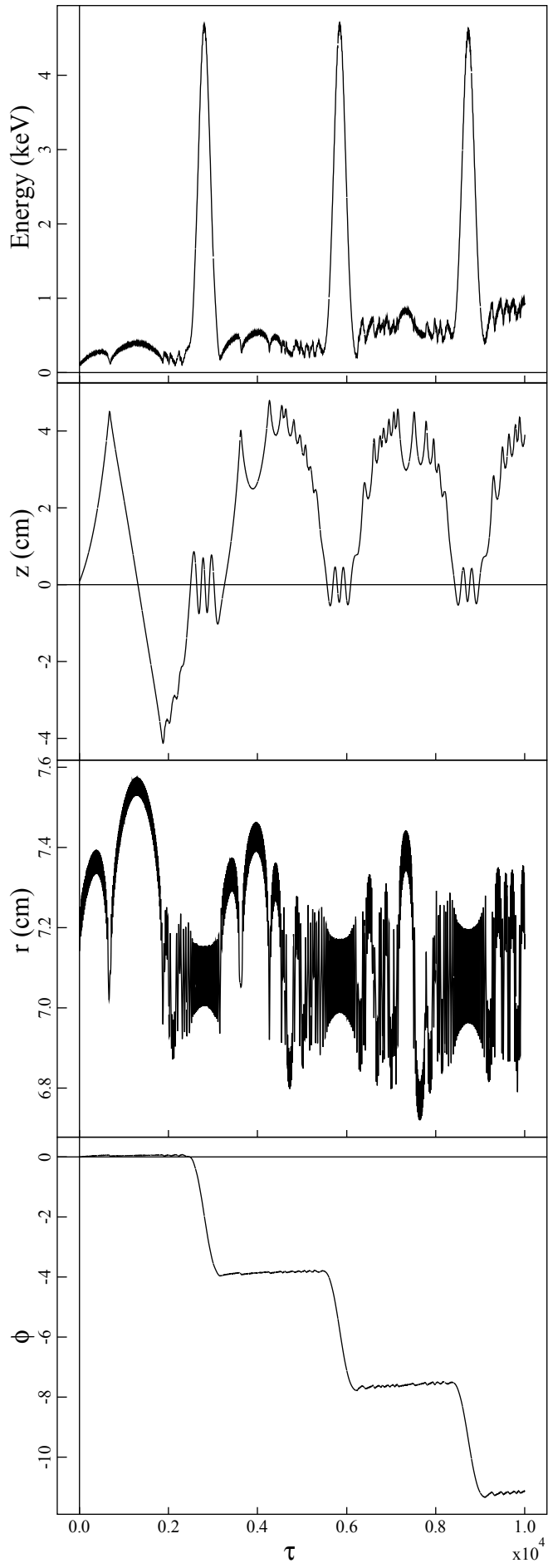
References

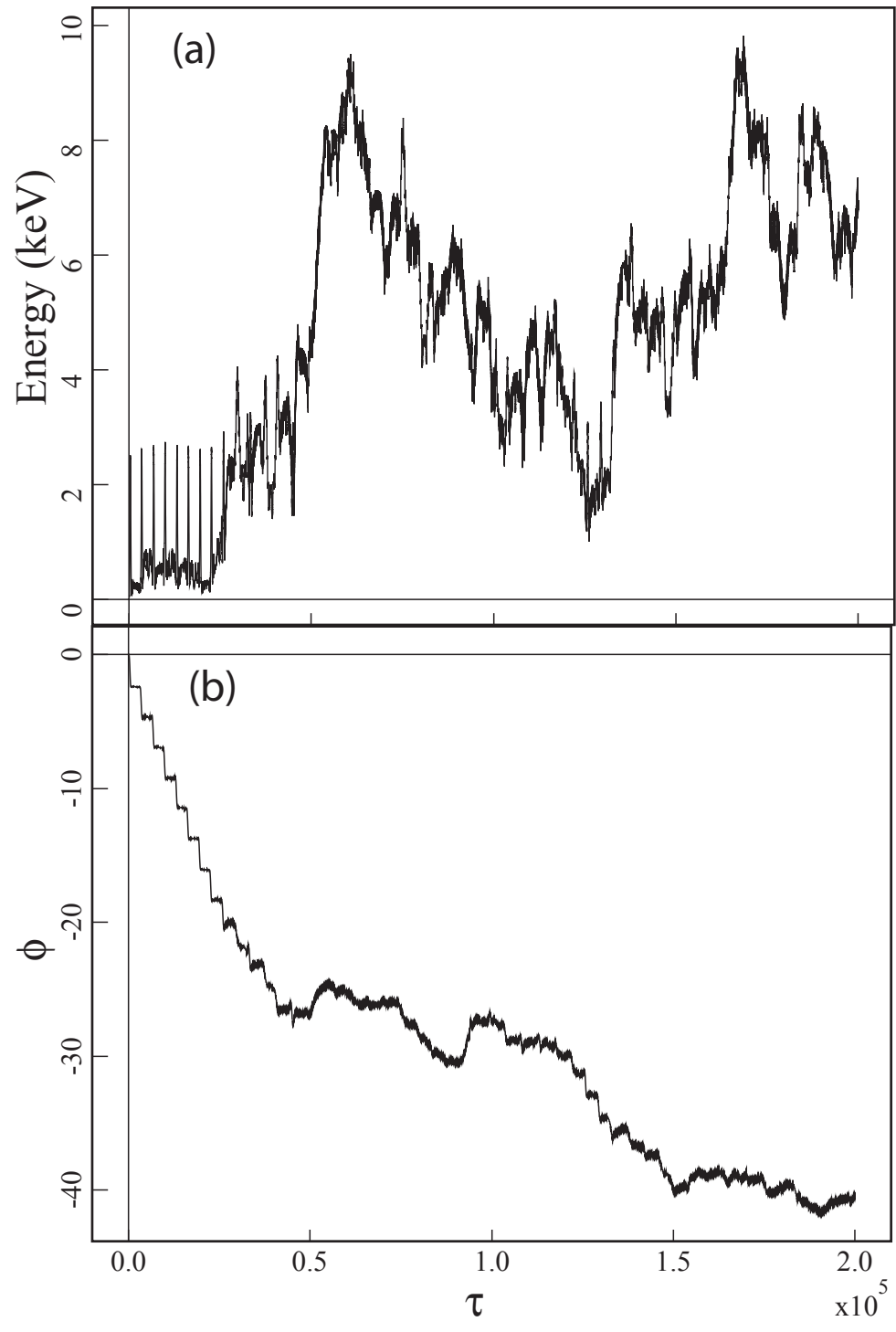
1. S.A. Cohen and A.H. Glasser, Phys. Rev. Lett. **85**, 5114 (2000).
2. S.A. Cohen and R.D. Milroy, Phys. Plasmas **7**, 2539 (2000).
3. D.C.Barnes, M. Binderbauer, R.D. Brooks, et al., Fusion Technology **30**, 116 (1996).
4. J.T. Slough and K. E. Miller, Phys. Plasmas **7**, 1945 (2000).
5. R.D. Milroy, Phys. Plasmas **7**, 4135 (2000).
6. A.L. Hoffman, Nucl. Fusion **40**, 1523 (2000).
7. A. Hassam, R. Kulsrud, R.J. Goldston et al., Phys. Rev. Lett. **83**, 2969 (2000).
8. T.W. Speiser, J. Geophys. Res. **70**, 4219 (1965).
9. A. C. Hindmarsh, “**ODEPACK, A Systematized Collection of ODE Solvers**”, in *Scientific Computing*, R. S. Stepleman et al., Editors (North-Holland, Amsterdam, 1983), pp. 55-64.
10. H. Goldstein, *Classical Mechanics*, 2nd ed., (Addison-Wesley, Reading, MA, 1980).
11. L.S. Solov’ev, Rev. Plasma Phys. **6**, 239 (1976).
12. W.N. Hugrass, J. Plasma Phys. **28**, 369 (1982).
13. M.Y. Yang and G.H. Miley, Nucl. Fusion. **79**, 39 (1979).
14. W.N. Hugrass and I. R. Jones, J. Plasma Physics **29**, 155 (1983).
15. H.A. Blevin and P.C. Thonemann, Nucl. Fusion: 1962 Supplement, Part 1, 55.
16. A.L. Hoffman, Phys. Plasmas **5**, 979 (1998).
17. M. Yamada, H. Ji, S. Hsu, et al., Phys. Rev. Lett. **78**, 3117 (1997).

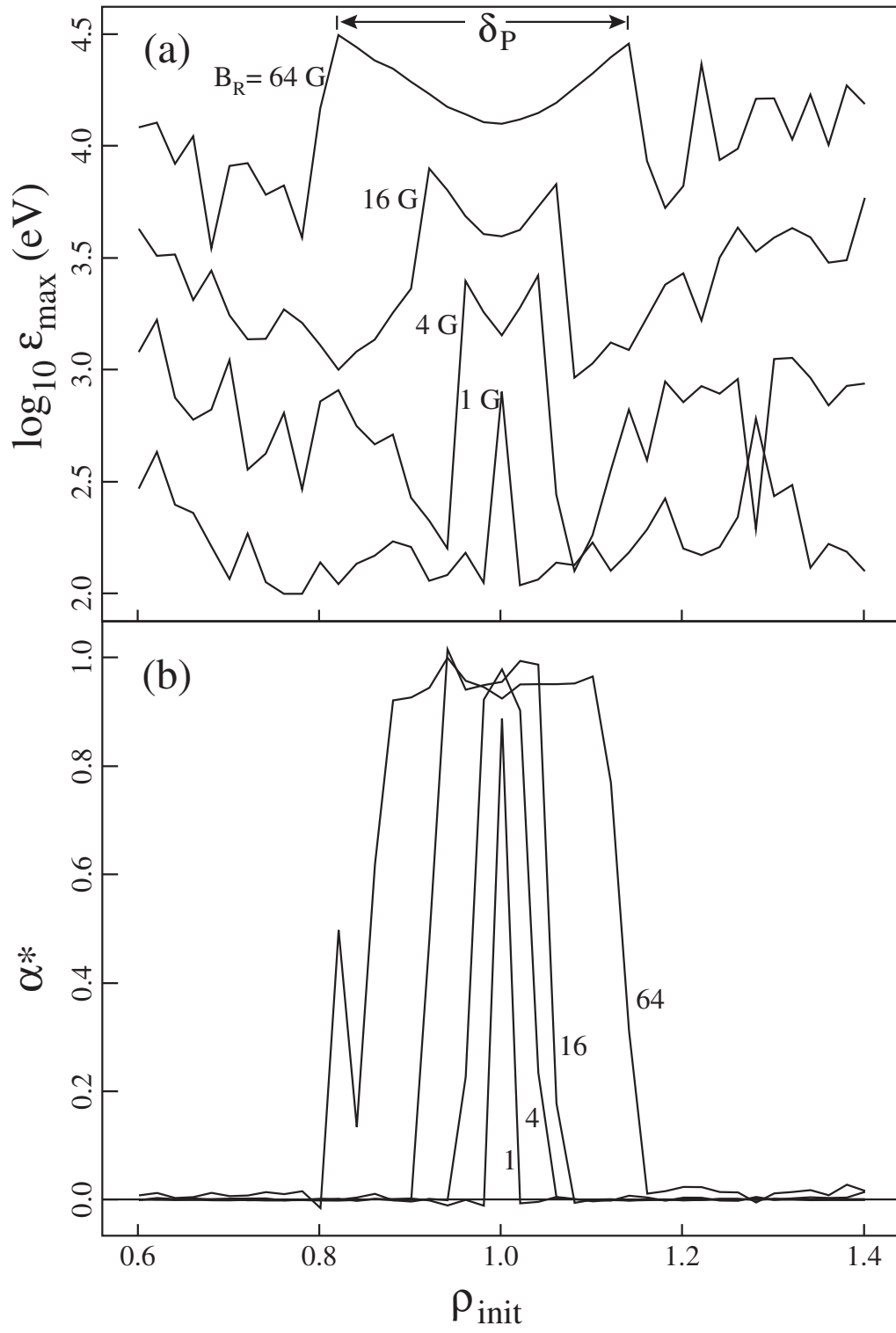
Figure captions

1. Calculated electron energy as a function of scaled dimensionless time, $\tau = \omega_{ce}t/2\pi$ in an FRC with $B_a = 2 \times 10^4$, $r_s = 10$ cm and $\kappa = 5$, for odd-parity RMFs with $\omega_R/\omega_{ce} = 2 \times 10^{-4}$ and $B_R = 20$ G.
2. Calculated electron a) energy, b) axial z , c) radial r , and d) azimuthal ϕ positions, on an expanded τ scale from Fig.1. The energy spikes are coincident with orbits near the O-point line and large negative-going steps in ϕ .
3. a) Electron energy *vs.* τ in the FRC for RMF_o with $\omega_R/\omega_{ce} = -2 \times 10^{-4}$ and $B_R = 20$ G. Spikes are seen at at low energy, < 4 keV. b) Azimuthal position *vs.* τ . When spikes occur, the azimuthal speed is close to that of the RMF_o, but the diirections of motion are opposite.
4. a) Maximum electron energy attained, \mathcal{E}_{\max} , *vs.* initial normalized electron radial position ρ_{init} , at $\omega_R/\omega_{ce} = 2 \times 10^{-4}$ for 4 values of B_R : 1, 4, 16, and 64 G. The duration of each RMF_{1,13} run was $\tau = 3 \times 10^4$. b) α^* , ratio of time-averaged electron azimuthal angular velocity to ω_R , *versus* ρ_{init} .









External Distribution

Plasma Research Laboratory, Australian National University, Australia
Professor I.R. Jones, Flinders University, Australia
Professor João Canalle, Instituto de Fisica DEQ/IF - UERJ, Brazil
Mr. Gerson O. Ludwig, Instituto Nacional de Pesquisas, Brazil
Dr. P.H. Sakanaka, Instituto Fisica, Brazil
The Librarian, Culham Laboratory, England
Library, R61, Rutherford Appleton Laboratory, England
Mrs. S.A. Hutchinson, JET Library, England
Professor M.N. Bussac, Ecole Polytechnique, France
Librarian, Max-Planck-Institut für Plasmaphysik, Germany
Jolan Moldvai, Reports Library, MTA KFKI-ATKI, Hungary
Dr. P. Kaw, Institute for Plasma Research, India
Ms. P.J. Pathak, Librarian, Institute for Plasma Research, India
Ms. Clelia De Palo, Associazione EURATOM-ENEA, Italy
Dr. G. Grosso, Instituto di Fisica del Plasma, Italy
Librarian, Naka Fusion Research Establishment, JAERI, Japan
Library, Plasma Physics Laboratory, Kyoto University, Japan
Research Information Center, National Institute for Fusion Science, Japan
Dr. O. Mitarai, Kyushu Tokai University, Japan
Library, Academia Sinica, Institute of Plasma Physics, People's Republic of China
Shih-Tung Tsai, Institute of Physics, Chinese Academy of Sciences, People's Republic of China
Dr. S. Mirnov, TRINITI, Troitsk, Russian Federation, Russia
Dr. V.S. Strelkov, Kurchatov Institute, Russian Federation, Russia
Professor Peter Lukac, Katedra Fyziky Plazmy MFF UK, Mlynska dolina F-2, Komenskeho
Univerzita, SK-842 15 Bratislava, Slovakia
Dr. G.S. Lee, Korea Basic Science Institute, South Korea
Mr. Dennis Bruggink, Fusion Library, University of Wisconsin, USA
Institute for Plasma Research, University of Maryland, USA
Librarian, Fusion Energy Division, Oak Ridge National Laboratory, USA
Librarian, Institute of Fusion Studies, University of Texas, USA
Librarian, Magnetic Fusion Program, Lawrence Livermore National Laboratory, USA
Library, General Atomics, USA
Plasma Physics Group, Fusion Energy Research Program, University of California at San
Diego, USA
Plasma Physics Library, Columbia University, USA
Alkesh Punjabi, Center for Fusion Research and Training, Hampton University, USA
Dr. W.M. Stacey, Fusion Research Center, Georgia Institute of Technology, USA
Dr. John Willis, U.S. Department of Energy, Office of Fusion Energy Sciences, USA
Mr. Paul H. Wright, Indianapolis, Indiana, USA

The Princeton Plasma Physics Laboratory is operated
by Princeton University under contract
with the U.S. Department of Energy.

Information Services
Princeton Plasma Physics Laboratory
P.O. Box 451
Princeton, NJ 08543

Phone: 609-243-2750
Fax: 609-243-2751
e-mail: pppl_info@pppl.gov
Internet Address: <http://www.pppl.gov>